Ab Initio Molecular Dynamics Studies of the Liquid−Vapor Interface of an HCl Solution†

Hee-Seung Lee*

Department of Chemistry and Biochemistry, University of North Carolina, Wilmington, North Carolina 28403

Mark E. Tuckerman*

Department of Chemistry and Courant Institute of Mathematical Sciences, New York University, New York, New York 10003

Received: October 18, 2008; Revised Manuscript Received: December 16, 2008

Ab initio molecular dynamics is used to investigate the propensity of the hydronium ion for the interface of an HCl solution containing 1 HCl and 96 water molecules in a slab geometry. Unconstrained trajectories in the NVT and NVE ensemble reveal a clear preference of the hydronium ion for the interfacial region and several qualitative spectral features of interfacial hydronium ions. Orientational distribution functions indicate that the C_3 axis of the hydronium is tilted with respect to the surface normal, thereby allowing surface proton transfer reactions to occur. Finally, constrained simulations combined with thermodynamic integration are used to compute the potential of mean force for the transfer of the hydronium from the bulk to the interface and into the gas phase as a pure H_3O^+. The potential of mean force is found to exhibit a shallow free energy minimum of roughly 1.3 kcal/mol with respect to the bulk, in good agreement with very recent calculations based on polarizable force fields and empirical valence bond potentials.

I. Introduction

Chemistry at the liquid−vapor interface of inorganic salt and acidic and basic solutions plays an important role and has far-reaching consequences in areas ranging from cell biology to atmospheric chemistry. For example, chlorine ions on an aerosol surface are believed to catalyze an important step in ozone depletion in the stratosphere,[1,2] but a detailed understanding of the uptake process and the subsequent heterogeneous chemistry on the surface of an aerosol has yet to be gained.

The structural characteristics of the liquid−vapor interfaces of water and ionic solutions have been studied experimentally by various groups[3−16] over the past 10 years. The elucidation of the microscopic structure of such interfaces is due to the emergence of surface specific techniques, such as vibrational sum frequency generation (VSFG) spectroscopy,[3,16−20] X-ray absorption (XAS) spectroscopy,[21,22] and second harmonic generation.[23,24] The VSFG spectrum of neat water has three main features: a sharp and intense peak at 3700 cm^{-1} and broader peaks at 3400 and 3200 cm^{-1}, which are often referred to as liquidlike and icelike bands, respectively.[3] The peak at 3700 cm^{-1} has been assigned unambiguously to the vibration of an OH bond that is not involved in the hydrogen bonding network and protrudes into the vapor phase. This OH bond is often called a "dangling OH" or "free OH" bond. The assignment and interpretation of the other two peaks, however, are not as clear as the free OH peak. For example, Richmond and co-workers[7,13] assigned the lower frequency side to the tetrahedrally (or strongly) coordinated water and the higher frequency side to the uncoupled donor OH vibration of water with the other OH bond dangling. Allen and co-workers[9,10,14] attributed the peak at 3400 cm^{-1} to the asymmetric tetrahedrally coordinated water and the peak at 3200 cm^{-1} to the DAA (single-donor, double-acceptor) species at the interface. Very recently, Shen and co-workers[20] developed a phase-sensitive VSFG technique and directly measured the real and imaginary parts of resonance signals, which provide more detailed information than the square of total intensity alone. They interpreted the low frequency region of spectrum as a sum of three contributions: donor OH bonds from DAA and DDA species in the interface (3450∼3700 cm^{-1}), asymmetrically bonded DDAA species (3200∼3450 cm^{-1}), and symmetrically bonded DDAA species (below 3200 cm^{-1}).

The impact of hydronium ions (H_3O^+) in acidic solution on the VSFG spectrum is, however, more elusive and is not entirely understood yet. One of the outstanding questions to be answered concerns the propensity of hydronium ions for the surface and the physical origin of the differences between VSFG spectra of water and acid solutions. Upon the addition of acid to neat water, the intensity of each peak in the VSF spectrum of neat water changes rather dramatically. For instance, Richmond and co-workers[13] reported that five features are buried under the VSF spectrum of HCl solution based on their isotopic dilution experiment. These peaks are centered at 3200, 3350, 3453, 3525, and 3700 cm^{-1}. The enhancement of the low frequency region (3200 and 3350 cm^{-1}) was interpreted as a direct contribution from the OH stretching of hydronium or Zundel cations as well as the effect of a strong electrostatic interaction between hydrated protons and water molecules. In addition, the new feature at 3525 cm^{-1} was attributed to the OH stretching by water molecules solvating hydronium ions on the surface. In contrast, Allen and co-workers[10] fitted the VSF spectra of an HCl solution with a different set of discrete peaks and concluded that the enhancement of the 3200 cm^{-1} peak is the result of the VSFG response from hydrated protons. They also found that the intensity of the 3700 cm^{-1} peak is significantly reduced in acidic solutions. Most recently, Shen and co-workers[16] reported the phase-sensitive VSF spectrum of an HCl solution and interpreted the spectrum without the ambiguity associated with the spectral fitting. Based on the imaginary part

† Part of the "Max Wolfsberg Festschrift".

* To whom correspondence should be addressed.

10.1021/jp809236c CCC: $40.75
Published on Web 02/05/2009

of the VSF signal, they clearly showed that the hydronium ion prefers to be located on the surface. In addition, they found (1) that the spectrum above 3500 cm^{-1} hardly changes upon addition of acid, which indicates that the total population of DAA and DDA species on the surface is unchanged, (2) that the enhancement between ∼3200 and ∼3500 cm^{-1} is due to the reorientation of DDAA molecules around the interface caused by the presence of hydronium on the surface, and (3) that the OH stretch frequency of hydrated protons should be below 3250 cm^{-1}.

On the theoretical side, the interfacial properties of acidic and basic solutions have been studied far less than bulk solutions for several reasons. First, conventional force fields are unable to treat the chemical bond breaking events associated with the Grotthuss structural diffusion mechanism of hydronium and hydroxide ions in water. Second, as was shown by Mundy and Kuo,[25] large system sizes are needed to have a proper description of both the interface and bulk region, and these are just at the limit of what can be adequately treated using modern *ab initio* molecular dynamics methods. Specific force-field models can be designed to account for the Grotthuss mechanism, and among the few theoretical studies of acidic solution, Voth and coworkers[26] carried out an empirical valence bond (EVB)[27−30] study of an HCl solution in a slab configuration. They found that the hydronium ion is preferentially located on the surface with the oxygen lone pair electrons directed away from the bulk. The physical origin of this preferred location and the orientation of hydronium were deduced from the nature of hydrogen bonds involving a hydronium ion. Since hydronium ions possess a positive charge, the hydronium oxygen is a poor hydrogen bond acceptor. Consequently, it tends to disrupt the regular hydrogen bonding network when present in the bulk. By migrating to the surface with the oxygen lone pair facing the vacuum, the hydronium ion can still donate all three hydrogens to neighboring water molecules and form an eigen cation ($H_9O_4^+$) without strongly perturbing the hydrogen bonding network, as also suggested in very recent phase-sensitive VSFG measurements.[16]

Prior to this EVB study, Dang[31] had reported the potential of mean force (PMF) for transferring the hydronium from the bulk across the interface of an acidic solution using a polarizable model[32] (which, nevertheless, is unable to account for the Grotthuss mechanism). This model leads to a very flat free energy profile from the bulk to the interface with possibly a shallow minimum or slight repulsion, obtained from constrained simulations in the forward and reverse directions, respectively. A more recent simulation[33] with a similar protocol, however, showed a shallow minimum (∼0.7 kcal/mol) around the interface. Very recent calculations of the PMF using the empirical valence bond approach for slab[34] and droplet[35] configurations, the former employing a more refined EVB model,[30] yield free energy minima at the Gibbs dividing surface for the hydronium ion of 1.8 and 2.4 kcal/mol, respectively.

Although the aforementioned studies have provided valuable insights into the structure of hydronium at the interface of an acidic solution, questions regarding the effect of the hydronium ion on the VSFG spectrum are not fully answered yet, and a quantitative understanding of the hydronium propensity for the interface (based, for example, on the potential of mean force) is only beginning to emerge. The validity of empirical potential models for treating the interface of acidic/basic solutions also needs to be confirmed at a higher level of theory. To this end, we have performed extensive *ab initio* molecular dynamics (AIMD) simulations of the liquid−vapor interface of an HCl solution, which provide a detailed microscopic-level window into the interfacial properties of the solution. The computational protocol in the present work employs Car−Parrinello type AIMD (CPAIMD),[36] in which the electronic structure of the system is represented within the density functional theory (DFT)[37] with the BLYP[38,39] exchange-correlation functional. In this paper, the propensity of the hydronium ion for the interface and its effect on the surface spectra and local structure of water at the surface are investigated.

II. Methodology

In the present study, all simulations were carried out using the Car−Parrinello *ab initio* molecular dynamics (CPAIMD) approach[36,40,41] as implemented in the PINY_MD code.[42] The electronic structure was represented within the Kohn−Sham (KS) density functional formalism[37,43,44] using the BLYP[38,39] generalized gradient approximation (GGA) for the exchange-correlation functional. It has been shown that the BLYP functional can reasonably describe the properties of aqueous systems.[45−56] The KS orbitals were expanded in a plane wave basis set at the Γ point up to an energy cutoff of 70 Ry. Core electrons were not treated explicitly; rather, atomic pseudopotentials of the Troullier and Martins (TM) type[57] were used. In the CPAIMD approach, the energy functional is not minimized explicitly at each MD step. Instead, the CP approach uses an adiabatically decoupled fictitious propagation scheme to advance electronic orbitals at each time step from one nuclear configuration to the next, thereby allowing atomic forces to be computed "on-the-fly" as the simulation proceeds. Because atomic forces are computed from the electronic structure, bond breaking and forming processes can be treated explicitly, which is crucial to study proton transport through aqueous media.

The present AIMD simulations contain 96 water molecules and 1 HCl molecule in a slab geometry. The reciprocal space approach of Minary et al.[58] was employed to explicitly treat the surface boundary conditions. The necessity of rigorous implementation of surface boundary conditions in the simulations of liquid−vapor interfaces was recently discussed by Mundy and Kuo.[25] The size of the simulation cell was 12.50 × 12.50 × 46.67 Å, which allows approximately 28 Å of vacuum between two neighboring slabs. While we expect finite-size effects with this system size,[25] as we will discuss later, we do obtain a reasonable description of the bulk region, on average, a stable interface when proper surface boundary conditions are employed,[58] and a reasonable potential of mean force for the transfer of the H_3O^+ from the bulk across the interface.

For all CPAIMD simulations, a time step of 0.1 fs along with the fictitious mass parameter of 875 au was employed. In order to reduce nuclear quantum effects, which are already expected to be small based on *ab initio* path-integral studies of the hydrated proton,[48] the deuterium mass was used for hydrogen. Therefore simulations were performed using 96 D_2O and 1 DCl rather than 96 H_2O and 1 HCl. This mass assignment does not affect any structural properties, such as radial distribution functions, but does alter the dynamical properties of the system, such as spectra. Despite this mass assignment, our notation will be "H" instead of "D".

A constant temperature (NVT) simulation of the 96 H_2O/HCl system was performed, starting from a structure with the hydronium midway between the interface and the center of the slab. To control the temperature, a Nosé−Hoover chain thermostat was attached to each degree of freedom.[59] This unconstrained simulation was carried out for 20 ps, and the average temperature during the simulation was 300 K. The trajectory from this simulation clearly shows the preferential

location of hydronium within liquid slab. In order to quantify the relative propensity of hydronium ions for the surface, it is necessary to estimate the potential of mean force (PMF) for the transfer of H_3O^+ from the bulk across the interface from a CPAIMD trajectory. However, as will be shown in section III, the hydronium is mostly located on the surface, which leads to poor sampling of the bulk region. Therefore, we performed thermodynamic integration calculations[60,61] and computed the free energy profile for the hydronium transfer process. The free energy difference ΔF between slab configurations for which the hydronium ion is located at z and z_s, respectively, is given by

$$\Delta F(z) = F(z) - F(z_s) = -\int_{z_s}^{z} \langle f_z(z') \rangle \, dz' \qquad (1)$$

where $f_z(z')$ is the z component of total force on the hydronium ion when it is located at $z = z'$, and the z axis is taken to be perpendicular to the interface. In eq 1, z_s can be regarded as a reference point taken to be the bulk region of the system in the present study. Since eq 1 requires the z component of the force averaged over a canonical ensemble, constrained CPAIMD simulations with the z coordinate of the hydronium ion center of mass fixed at particular values, ranging from $z = 1$ to 11 Å with an increment of 1.0 Å, were used. In each constrained simulation, proton transfer is suppressed by constraining the three OH bonds of the hydronium to a value of 1.062 Å, which is the average O—H distance of a hydronium obtained from an unconstrained simulation. Additional simulations were performed for the hydronium ion around the interface: $z = 7.5$, 8.5, and 9.5 Å. In total, 14 constrained CPAIMD simulations were performed at 305 K for 5 ps at each ion position. The z component of the force exerted on the hydronium ion was averaged during the last 4 ps of each CPAIMD simulation. The total accumulated simulation time performed in the present work for the 96 H_2O/HCl system is, therefore, 90 ps. We note in passing that the constrained trajectories were not used for the analysis of slab structure reported in section III, as each of the 14 constrained simulations were initiated from similar initial starting configurations and do not significantly improve the sampling. Therefore, we only used the data obtained from a 20 ps long unconstrained simulation to analyze the structure of liquid slab. All reported CPAIMD simulations were performed on the Cray-XT ("BigBen") at the Pittsburgh supercomputing center.

III. Results and Discussion

In the present AIMD simulations of the 96 H_2O + HCl system with surface boundary conditions (see Figure 1 for a snapshot), the thickness of liquid slab is ~18 Å, which is rather small. It has been argued that bulk liquid water behavior is recovered at 10 Å below the surface.[62] This lead the authors of ref 63 to use a large simulation cell (216 water molecules) in their state-of-the-art AIMD study of the liquid—vapor interface of water. The simulation was, by necessity, short (5 ps), and even such a large system appears to generate a relatively thin interfacial region. In fact, it is expected that all current *ab initio* MD simulations of interface suffer from finite-size effects to some degree, possibly more than they do in bulk simulations. It was shown by Yeh and Hummer[64] that true bulk limit cannot be reached unless the system includes a few thousands of water molecules in bulk simulations. The smaller system size (96 H_2O rather than 216 H_2O) employed in this study is one that can be used to generate a sufficiently long simulation needed for quantitative results on currently available computing resources. While we realize that this is a necessary compromise, we were able to perform a total of 90 ps of CPAIMD on the present system. To verify that the system size is adequate for the purpose of the present work, we evaluated the stability of the liquid slab system employed here before analyzing the CPAIMD data. In particular, the system should have a stable bulklike region in the slab center. Note that, as shown below, the properties of liquid slab found in the present work are qualitatively similar to those obtained for the 216 water system of Kuo and Mundy.[63] Moreover, we are able to capture the bulk and interfacial solvation structures of the hydronium ion using the 96 water system employed here, and we believe this should lead to a reasonable prediction of the potential of mean force.

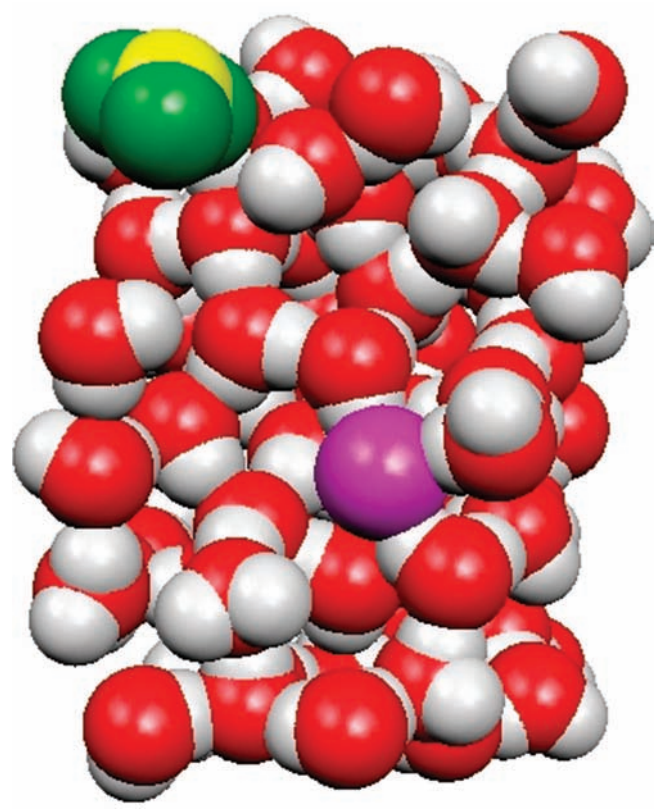

Figure 1. Snapshot of the 96 H_2O + HCl system from the CPAIMD simulation. Color scheme is as follow: hydronium oxygen = yellow, hydronium hydrogen = green, purple = chlorine.

Figure 2a depicts the computed density profile obtained from the 20 ps unconstrained CPAIMD simulation. Although the "top" and "bottom" surfaces of the slab are chemically distinct (as shown in Figure 1, only one of them is populated by hydronium), there is practically no difference in the density of water between the upper and lower portions of the liquid slab. Therefore, the average density between the two portions of the liquid slab was taken to enhance the sampling. The figure shows that the density profile exhibits large fluctuations. The large fluctuations in the density profile are due to the short simulation time and the finite-size effects mentioned earlier. It should be noted, however, that similar behavior in the density profile was also observed in a simulation with 216 water molecules.[63,65] The density profile reported by Kuo and Mundy,[63] however, exhibits a thicker interfacial region, which indicates that finite-size effects are more prominent in our system, as expected. The interfacial thickness parameter, δ, obtained from a fit of the density profile to a hyperbolic tangent form (Figure 2a) is only 0.25 Å, whereas $\delta = 0.786$ Å was reported in ref 65. In order to assess whether the 96 H_2O + HCl system has a resonable bulklike region, the

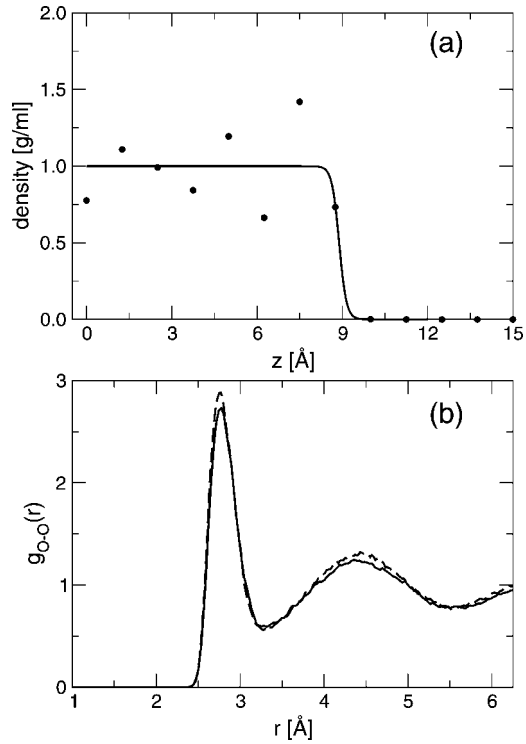

Figure 2. (a) Density profile for the 96 water molecules in slab configuration obtained from the 20 ps unconstrained NVT simulation (closed circle). The density profile was fit (solid line) to a hyperbolic tangent function of the form $\rho(z) = (1/2)(\rho_l + \rho_r)\tanh((z - z_{GDS})/\delta)$, where z_{GDS} is the location of the Gibbs dividing surface. (b) Oxygen−oxygen radial distribution function (RDF) for the water molecules found in the interior region (4 Å thick) of the slab (solid line). The RDF from fully periodic simulation of 64 water molecules (density = 0.978 g/mL) is overlapped for comparison (dashed line).

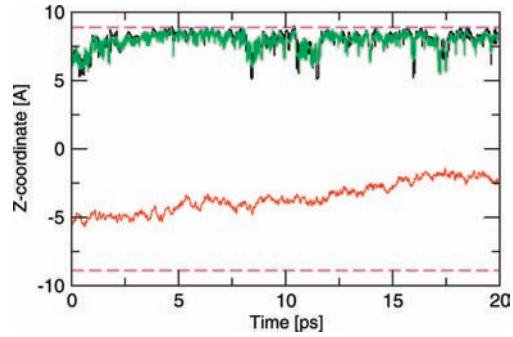

Figure 3. Instantaneous z coordinates (normal to the surface) of hydronium oxygen (black), proton (green), and chlorine (red) observed during the 20 ps unconstrained NVT simulation of the 96 H_2O + HCl interfacial system. The dashed line indicates the location of the Gibbs dividing surface defined in Figure 2a.

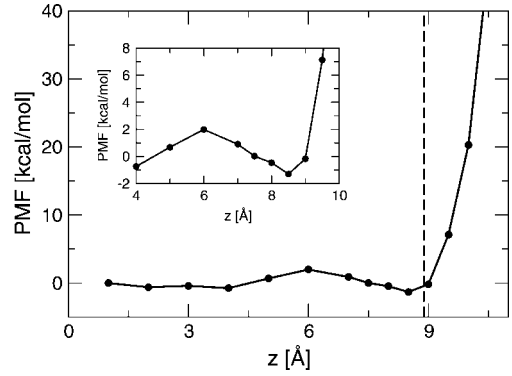

Figure 4. Potential of mean force (PMF, or free energy difference) for transferring a hydronium ion across the liquid slab with 96 water molecules at 305 K. As a reference point, $F(z_s)$ in eq 1 was chosen as the free energy in the bulk region. The dashed line indicates the location of the Gibbs dividing surface. The inset shows the PMF on a finer y scale.

radial distribution function (RDF) for the oxygen atoms in the interior region of the slab was computed. Figure 2b shows the oxygen−oxygen RDF for oxygen atoms found within a 2 Å region from the center of the liquid slab (4 Å thick slab). Since there is still some uncertainty about the bulk density of liquid water predicted using the BLYP functional,[66−68] particularly concerning basis-set size effects, we assumed that the average density of the 4 Å thick slab in the middle represents the bulk density in order to determine $g_{OO}(r)$. For comparison, the $g_{OO}(r)$ obtained from a 10 ps simulation of a periodic bulk system with 64 water molecules is overlapped. It is clear that the first and second solvation shell structures obtained from the bulk region of the interfacial system are similar to those from a fully periodic calculation (300 K, 0.979 g/mL), implying that the present 96 H_2O + HCl system supports a well-defined bulk region, on average.

As a demonstration of the preferred location of the hydronium ion in the unconstrained AIMD trajectory, the z coordinates (normal to the surface) of the excess proton, the hydronium oxygen, and the chlorine ion are plotted in Figure 3 as a function of the simulation time. The origin of the z axis is taken to be the center of the slab. In order to locate the hydronium in each configuration, the following algorithm is used: Each hydrogen is first assigned unambiguously to its closest oxygen; following this assignment, the number of hydrogens associated with each oxygen is determined. The oxygen with three associated hydrogens is taken to be the hydronium defect and is denoted O*. The starting configuration for the simulation had the hydronium ion midway between the interface and the center of the liquid slab. As seen in Figure 3, the hydronium ion moves to the surface within a few picoseconds. Although the actual dynamics is not preserved in the present NVT simulation, the trajectory does reveal that the hydronium has a clear preference for the surface. Indeed, once the hydronium moves to the surface, it stays on the surface throughout the simulation. As indicated by the trajectory of the excess proton, the hydronium on the surface is dynamically disordered due to frequent transfers of the excess proton to neighboring surface water molecules. Although less frequent, the excess proton is sometimes transferred to a water molecule just below the surface. However, when this occurs, the hydronium returns to the surface almost immediately.

The propensity of the hydronium ion for the liquid−vapor interface is further supported and quantified by the potential of mean force (PMF) for transferring the hydronium ion from the bulk across the interface. Figure 4 shows the PMF (or free energy difference profile) as a function of z from the bulk across the Gibbs dividing surface (GDS) using the thermodynamic integration protocol described in the previous section. The free energy profile is relatively flat until the hydronium ion reaches the GDS, although we find a small barrier between the interface and the interior region of the slab. As the ion crosses the interface, there is a very shallow minimum around the dividing surface of approximately 2∼3 kcal/mol (the actual value we obtain is 1.3 kcal/mol with respect to the bulk and 3.4 kcal/mol with respect to the maximum around $z = 6$ Å.) The free energy increases rapidly after the minimum, indicating that the hydronium ion is in the gas phase. This result indicates that a small

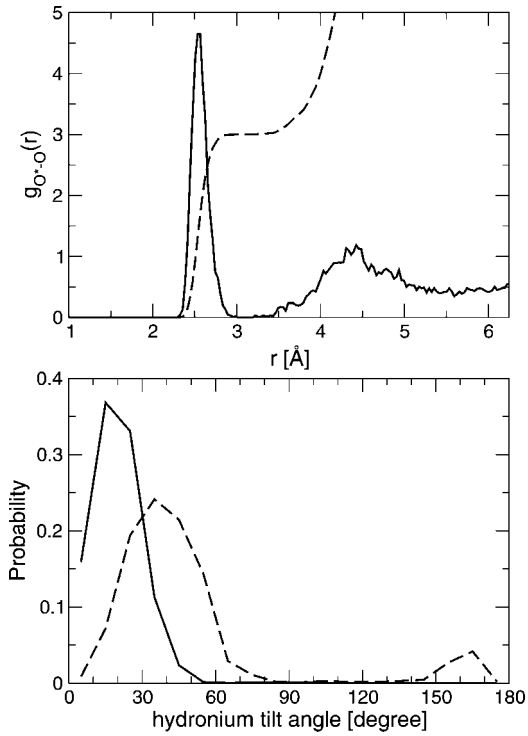

Figure 5. (top) Oxygen−oxygen RDF (solid line) for the hydronium ion on the surface. An entity is considered as a hydronium only if three O−H distances are within 0.1 Å. The running coordination number (dashed line) is also overlapped to show that hydronium donates three hydrogen bonds on the surface. (bottom) Orientation of hydronium on the top surface layer (solid line) and subsurface layer (dashed line) with respect to the surface normal. Angle zero means hydronium has an upright position with oxygen pointing to the vacuum and three hydrogens pointing to the bulk.

free energy difference is enough to create a strong propensity of hydronium for the interface. The free energy profile obtained in the present work from the constrained CPAIMD simulations is similar to that obtained by Dang,[31] in which the PMF for a given hydronium position was computed from 300 ps long classical MD simulation with a polarizable force field.[32] The classical MD results show no significant minimum in PMF around the interface and a weak oscillation in the interior region of the slab. However, more recent calculation by Wick and co-workers[33] with a similar force field showed that the PMF around the interface has a shallow minimum with the depth of ∼0.7 kcal/mol. The free energy minimum obtained here is also in good agreement with the value recently obtained by Voth and co-workers[26,30] from EVB simulations and by Köfinger and Dellago[35] using a water droplet sample.

The structure of hydronium ion on the interface was analyzed by calculating the O*O RDF of the hydronium on the surface (recall that O* refers to the hydronium oxygen) as well as the orientation of the hydronium ion on the surface. In this analysis, we consider a protonated water molecule as a hydronium ion only if all three OH bond distances are within 0.1 Å from each other; otherwise, it is considered as a Zundel ($H_5O_2^+$) cation. This definition of the hydronium ion ensures that the sampled hydronium ions have a symmetric structure (i.e., three equivalent OH bonds) and therefore the orientation of the hydronium can be defined unambiguously. Even with this rather strict criterion, more than 50% of the configurations have a symmetric hydronium during the 20 ps NVT simulation.

Figure 5 (top) shows $g_{O^*O}(r)$ obtained for the hydronium ions on the surface satisfying the aforementioned criterion. The coordination number of hydronium on the surface, which is obtained by integrating $g_{O^*O}(r)$ up to the first minimum, is 3. This indicates that all three OH bonds of the hydronium participate in the hydrongen bonding network on the surface. The orientation of the surface hydronium is also plotted as a function of the tilt angle θ. The θ in the figure is defined as the angle between the surface normal and the vector pointing from the center of the triangle made by three hydrogens to the hydronium oxygen O*. With this definition, $\theta = 0$ corresponds to the geometry where the hydronium is in an upright position with the oxygen atom pointing its lone pair straight into the vacuum. In general, the angular distribution for the hydronium ion on the surface shown in Figure 5 (bottom) agrees with the description provided by Voth and co-workers based on the EVB approach.[26] However, the average angle is around 20°, and the distribution extends to fairly large angles in the AIMD simulations, despite the restriction to symmetric hydronium ions. This distribution is consistent with the picture that one or possibly two OH bonds are parallel with the surface. This tilted hydronium geometry enhances proton transfer along the surface. When there is a proton transfer event along the surface, the defect structure must pass through a Zundel cation structure, and the O−H−O bond favors an orientation parallel to the surface. Therefore, a tilted hydronium with at least one OH bond parallel to the surface leads more readily to proton transfer than would a hydronium in a perfectly upright position with all three OH bonds pointing into the bulk. The water molecule that receives the proton should be properly solvated on the surface with both OH bonds donating hydrogen bonds, but without accepting hydrogen bonds from nearby water molecules. In this way, the water molecule is ready to receive a proton and become a properly solvated hydronium, as described in ref 48.

A proton transfer from the surface hydronium to a water molecule below the surface layer is not impossible, and we observed several such events during the 20 ps simulation. This behavior can be seen from the angular distribution of hydronium ions in the subsurface layer. Right after a proton transfer to subsurface water, the hydronium can have an upside-down orientation, which is reflected in the dashed line in Figure 5 (bottom). However, the proton transferred to a subsurface water returns to the surface within a picosecond.

The local structure of the hydrogen bonding network on the surface of liquid water and acid/base and salt solutions is also of great interest. In particular, the "single-donor" moiety, which has one dangling OH bond toward the vacuum, has been extensively studied by VSFG experiments.[3,7,69] Furthermore, a recent X-ray study[22] indicated that there even exists "acceptor-only" species on the surface of liquid water. While molecular dynamics simulations can provide detailed information on such species by counting the number of water molecules in different environments, the actual number of species with a particular hydrogen bonding environment depends on the definition of the hydrogen bond employed. However, the qualitative trend in the hydrogen bonding pattern between the bulk and its interface or between water and acid interfaces should be insensitive to the specific choice of the hydrogen bond definition.[65] Here, we adopted the "loose" hydrogen bond definition used by Kuo et al.[65] Specifically, the O−H···O angle should be greater than 140°, and the O···O distance should be smaller than 2.27 Å to be a hydrogen bond. A more strict definition of a hydrogen bond reduces the number of hydrogen bonds per water molecule, but the qualitative trend remains unaltered.[65]

Table 1 shows the hydrogen bond statistics for the water molecules in the interior and surface regions. Only the top

TABLE 1: Percentage of Water Molecules That Have the Specified Number of Donor and Acceptor Hydrogen Bonds in Three Different Regions of Liquid Slab Obtained from the 20 ps Unconstrained CPAIMD Simulation of the 96 H_2O + HCl System[a]

	no. of donors								
	interior			acid surface			water surface		
no. of acceptors	0	1	2	0	1	2	0	1	2
0	0.2	0.9	0.5	1.4	2.5	0.8	1.0	3.1	1.3
1	1.3	10.6	16.8	4.1	36.3	36.8	4.2	33.0	28.8
2	1.4	17.2	51.1	0.5	14.9	2.7	1.5	20.7	6.4

[a] Three different regions are "interior" (4 Å thick slab in the middle), "acid surface" (surface with hydronium), and "water surface" (surface without hydronium). A loose hydrogen bond definition was adopted: H−O···H angle larger than 140° and O···O distance smaller than 2.27 Å.

surface layers (far right and left points in Figure 2a with $|z| > 8.125$ Å) were considered as the surface region, whereas the 4 Å thick slab in the middle, which was used to generate the bulk RDF in Figure 2b, was considered as the interior region. We report the results for "top" and "bottom" surfaces separately in Table 1 because the hydronium was located only on the top surface. Therefore, the bottom surface may be regarded as a neat water surface. The hydrogen bond population in the interior region shows that fourfold coordination is dominant, ensuring the bulklike nature of the interior region in our simulation. As water molecules go from the interior to the surface region, the species with DA, DDA, and DAA configurations become dominant, where "D" and "A" refer to donor bond and acceptor bond, respectively. The numbers of single-donor and acceptor-only species can be calculated by summing over each column under 1D and 0D, respectively. Although acceptor-only species do exist, their contribution (<10%) seems to be negligiable in both the water surface and the acid surface.

One of the changes found in the VSFG spectra upon adding acid to water is a noticeable decrease in the intensity of the peak at 3700 cm^{-1}.[9,10] The observed decrease of the free OH peak was interpreted as a fingerprint indicating a decrease in the population of the free OH bonds at the acid interface compared to that of a neat water surface. If we compare the total populations of 1D species on the acid surface (top surface) and water surface (bottom surface), we observe only a minor decrease in the free OH population as we go from the water to the acid surface. This finding is generally consistent with the recent phase sensitive VSF study of Shen and co-workers,[16] who observed a negligible decrease in the intensity of free OH peak. However, if we compare the DAA and DDA species, there is a significant increase in the DDA population and a decrease in the DAA population as we go from the water to the acid surface. The main driving force for such a change is the existence of hydronium ion on the acid surface. An analysis on the hydrogen bonding structure of hydronium ion on the acid surface reveals that the water molecules in the first solvation shell of the hydronium ion on the surface predominantly donate two hydrogen bonds but do not accept a hydrogen bond from nearby water molecules. More specifically, it was found that 82% of water molecules in the first solvation shell of the hydronium are DDA species. This indicates that the hydrogen bonding environment in the acid surface is different from that on the neat water surface due to the presence of hydronium ions on the surface. Therefore, hydronium ions on the surface indirectly influence the VSFG spectrum of aqueous solution, which is mainly reflected in the enhancement of the low frequency region of the VSF spectrum of acid solutions compared to that of neat water.

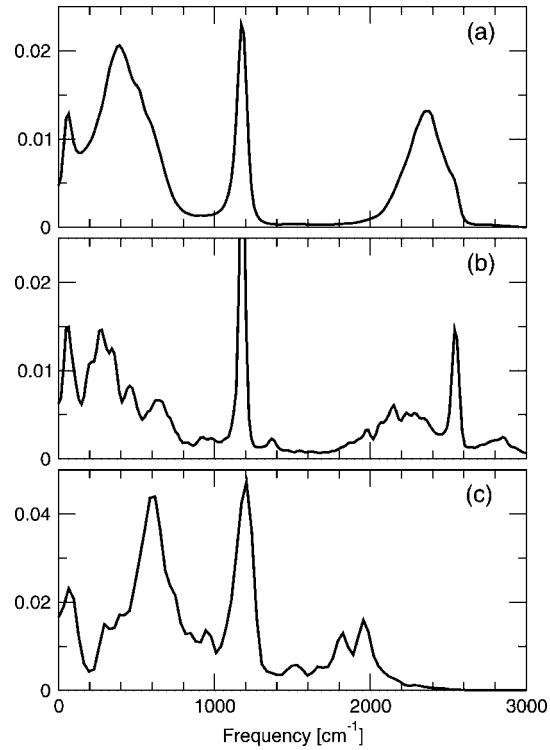

Figure 6. (a) Total power spectrum obtained from a constant energy simulation (NVE) of a 64 H_2O + HCl interfacial system. (b) Power spectrum of single water molecule on the surface with one dangling O−H bond. (c) Power spectrum of a hydronium ion on the surface.

We have also attempted to extract the spectroscopic signature of the hydronium ion on the surface by calculating the power spectrum of a single hydronium ion at the interface. However, due to the dynamic nature of hydronium ion, it is difficult to find a contiguous segment of trajectory of sufficient length to compute the hydronium only spectrum. Indeed, a very long simulation would be needed to obtain a sufficiently long trajectory with an uninterrupted hydronium ion, and such a simulation with 96 H_2O is prohibitively expensive. Therefore, we computed the power spectrum of a hydronium ion on the surface from constant energy (NVE) CPAIMD simulations of a 64 H_2O + HCl system. We found two 1 ps long trajectory segments that contain an intact hydronium ion without proton transfer. Since two spectra obtained from separate 1 ps trajectories look quite similar, we present the average of the two hydronium spectra in Figure 6c. We note that, although the system is small, the simulations are stable and the slab structure remains intact throughout the simulations. Although a slab consisting of 64 waters is likely too small to probe the slab structure, it should suffice for investigating the very local property of the O−H vibration of hydronium in the heterogeneous environment of the GDS. Admittedly, the analysis is rather qualitative, but it shows important characteristics also found in the VSFG spectrum.

Figure 6a shows the total power spectrum obtained from the velocity autocorrelation function of the NVE simulation for the 64 H_2O + HCl system. Note that the O−H stretching region appears at 2400 cm^{-1} due to the deuterium mass used for the hydrogens. Compared to the power spectrum of bulk water,[45] the stretching region is extended to higher frequencies, and a shoulder occurs around 2550 cm^{-1}. It is interesting to note that

the overall structure of the power spectrum in this frequency region is very similar to the IR and Raman spectra computed by Tobias and co-workers.[70] We also computed the power spectrum of a single water molecule on the surface that has one dangling OH bond for the majority of the simulation time. This water molecule was chosen from the bottom surface of the slab, which does not have the hydronium ion during the simulation. A single molecule power spectrum, which is shown in Figure 6b, has two main features at the stretching region: one broad feature at 2250 cm^{-1} and one sharp peak at 2550 cm^{-1}. The intense sharp peak is clearly due to the free OH vibration and nicely matches the shoulder in Figure 6a. Therefore, the shoulder seen at the higher frequency side of the O−H stretching region in Figure 6a can be identified as a dangling OH vibration. On the other hand, the broad feature in the power spectrum is due to the other OH bond participation in the hydrogen bonding, which is often called an "uncoupled donor OH" vibration.

In contrast to the water on the surface, the power spectrum of the hydronium on the surface has a distinctive feature. As shown in Figure 6c, the maximum in the O−H stretching region is more than 500 cm^{-1} red-shifted compared to the dangling O−H peak (recall that the power spectra in Figure 6 are for deuterated species). Although the quality of the hydronium spectrum is not as good as the others due to the short trajectories, it clearly indicates that the hydronium vibration mainly contributes to the spectrum below 2000 cm^{-1}, which corresponds to the tail end of the surface water power spectrum in Figure 6b. In the earlier VSFG studies of HCl solutions, the strong enhancement of the 3200 cm^{-1} peak (500 cm^{-1} below the free OH peak) in the VSF spectrum of acid solutions was attributed to the hydronium presence on the surface.[10,13] However, the result of the present CPAIMD simulation seems to be consistent with the more recent VSFG study,[14] which estimates that the hydronium OH stretch signal should be located below 3000 cm^{-1}, implying that the enhancement of the 3200∼3500 cm^{-1} region in the VSF spectrum of an acid solution is not the result of a VSF response of the hydronium OH stretch. Instead, the hydronium OH stretch signal is likely overlapping with the tail end of the OH stretching region in the VSF spectrum of the HCl solution. The phase sensitive VSF study by Shen and coworkers[16] also predicts that the VSF response from the hydronium OH stretch should be in the low frequency region, in the range of 3000∼3250 cm^{-1}.

IV. Conclusion

Ab initio molecular dynamics were employed to investigate the propensity of the hydronium ion for the interface of an HCl solution containing 1 HCl and 96 water molecules in a slab geometry with a proper treatment of the surface boundary conditions. While the system size is small compared to that recommended by Mundy and Kuo,[63] the interior region was shown to have, on average, the correct bulk structure, although large density fluctuations are observed. More importantly, a stable interface is maintained via the reciprocal-space screen function approach[58] for treating the two-dimensional periodicity of the system.

Unconstrained trajectories in the NVT ensemble reveal a clear preference of the hydronium ion for the interfacial region, and the potential of mean force $F(z)$ for the transfer of the hydronium from the bulk across the interface exhibits a shallow minimum of 1.3 kcal/mol at the interface, in good agreement with very recent MD simulations[33] using a polarizable force field and with empirical valence bond model calculations.[30,35] Orientational distribution functions computed from an unconstrained trajectory indicate that the C_3 axis of the hydronium is tilted with respect to the surface normal by approximately 20° with a fairly broad distribution about this average. The fact that the hydronium exhibits this tilt allows for surface proton transfer reactions.

A hydrogen bond population analysis shows that the presence of hydronium at the liquid−vapor interface can alter the hydrogen bond network at the surface, increasing DDA species but decreasing DAA species. However, the overall population of single-donor species on the acid surface was found to be relatively unchanged with respect to the neat water surface, a finding that is consistent with recent phase-sensitive VSFG measurements.[16] Furthermore, the computed power spectrum reveals that the contribution from the hydronium OH vibration overlaps with the tail end of the uncoupled OH peak of water, which indicates that the direct contribution from the hydronium to the enhancement of 3200 and 3400 cm^{-1} peaks in the VSFG spectrum of HCl solution is generally minor.

Acknowledgment. M.E.T. acknowledges support from NSF CHE-0310107 and NSF CHE-0704036. All calculations were made possible from an allocation on the Cray XT3 system ("BigBen") at the Pittsburgh Supercomputing Center.

References and Notes

(1) Molina, M. J.; Molina, L. T.; Kolb, C. E. *Annu. Rev. Phys. Chem.* **1996**, *47*, 327.
(2) Knipping, E. M.; Lakin, J. J.; Foster, K. L.; Jungwirth, P.; Tobias, D. J.; Gerber, R. B.; Dabdub, D.; Finlayson-Pitts, B. J. *Science* **2000**, *288*, 301.
(3) Du, Q.; Superfine, R.; Freysz, E.; Shen, Y. R. *Phys. Rev. Lett.* **1993**, *70*, 2313.
(4) Baldelli, S.; Schnitzer, C.; Shultz, M. J. *J. Chem. Phys.* **1998**, *108*, 9817.
(5) Baldelli, S.; Schnitzer, C.; Shultz, M. J. *Chem. Phys. Lett.* **1999**, *302*, 157.
(6) Schnitzer, C.; Baldelli, S.; Shultz, M. J. *J. Phys. Chem. B* **2000**, *104*, 585.
(7) Raymond, E. A.; Tarbuck, T. L.; Brown, M. G.; Richmond, G. L. *J. Phys. Chem. B* **2003**, *107*, 546.
(8) Raymond, E. A.; Richmond, G. L. *J. Phys. Chem. B* **2004**, *108*, 5051.
(9) Liu, D.; Ma, G.; Levering, L. M.; Allen, H. C. *J. Phys. Chem. B* **2004**, *108*, 2252.
(10) Mucha, M.; Frigato, T.; Levering, L. M.; Allen, H. C.; Tobias, D. J.; Dang, L. X.; Jungwirth, P. *J. Phys. Chem. B* **2005**, *109*, 7617.
(11) Petersen, P. B.; Saykally, R. J. *J. Phys. Chem. B* **2005**, *109*, 7976.
(12) Gopalakrishnan, S.; Liu, D. F.; Allen, H. C.; Kuo, M.; Shultz, M. J. *Chem. Rev.* **2006**, *106*, 1155.
(13) Tarbuck, T. L.; Ota, S. T.; Richmond, G. L. *J. Am. Chem. Soc.* **2006**, *128*, 14519.
(14) Levering, L. M.; Sierra-Hernandez, M. R.; Allen, H. C. *J. Phys. Chem. C* **2007**, *111*, 8814.
(15) Petersen, P. B.; Saykally, R. J. *Chem. Phys. Lett.* **2008**, *458*, 255.
(16) Tian, C.; Na, J.; Waychunas, G. A.; Shen, Y. R. *J. Am. Chem. Soc.* **2008**, *130*, 13033.
(17) Richmond, G. L. *Annu. Rev. Phys. Chem.* **2001**, *52*, 357.
(18) Ostroverkhov, V.; Waychunas, G.; Shen, Y. R. *Phys. Rev. Lett.* **2005**, *94*, 046102.
(19) Ji, N.; Ostroverkhov, V.; Chen, C. Y.; Shen, Y. R. *J. Am. Chem. Soc.* **2006**, *129*, 10056.
(20) Ji, N.; Ostroverkhov, V.; Tian, C. S.; Shen, Y. R. *Phys. Rev. Lett.* **2008**, *100*, 096102.
(21) Wilson, K. R.; Tobin, J. G.; Ankudinov, A. L.; Rehr, J. J.; Saykally, R. J. *Phys. Rev. Lett.* **2000**, *85*, 4289.
(22) Wilson, K. R.; Cavalleri, M.; Rude, B. S.; Schaller, R. D.; Nilsson, A.; Pettersson, L. G. M.; Goldman, N.; Catalano, T.; Bozek, J. D.; Saykally, R. J. *J. Phys.: Condens. Matter* **2002**, *14*, L221.
(23) Franken, P. A.; Weinreich, G.; Peters, C. W.; Hill, A. E. *Phys. Rev. Lett.* **1961**, *7*, 118.
(24) Petersen, P. B.; Saykally, R. J. *J. Phys. Chem. B* **2006**, *110*, 14060.
(25) Mundy, C. J.; Kuo, I.-F. W. *Chem. Rev.* **2006**, *106*, 1282.
(26) Petersen, M. K.; Iyengar, S. S.; Day, T. J. F.; Voth, G. A. *J. Phys. Chem. B* **2004**, *108*, 14804.
(27) Warshel, A.; Weiss, R. M. *J. Am. Chem. Soc.* **1980**, *102*, 6218.
(28) Schmitt, U. W.; Voth, G. A. *J. Chem. Phys.* **1999**, *111*, 9361.

(29) Day, T. J. F.; Soundachov, A. V.; Cuma, M.; Schmitt, U. W.; Voth, G. A. *J. Chem. Phys.* **2002**, *117*, 5839.
(30) Wu, Y.; Chen, H.; Wang, F.; Paesani, F.; Voth, G. A. *J. Phys. Chem. B* **2008**, *112*, 467.
(31) Dang, L. X. *J. Chem. Phys.* **2003**, *119*, 6351.
(32) Dang, L. X.; Chang, T. M. *J. Chem. Phys.* **1997**, *106*, 8149.
(33) Wick, C. D.; Kuo, I.-F. W.; Mundy, C. J.; Dang, L. X. *J. Chem. Theor. Comp.* **2007**, *3*, 2002.
(34) Iuchi, S.; Chen, H.; Paesani, F.; Voth, G. A. *J. Phys. Chem. B*, in press.
(35) Kofinger, J.; Dellago, C. *J. Phys. Chem. B* **2008**, *112*, 2349.
(36) Car, R.; Parrinello, M. *Phys. Rev. Lett.* **1985**, *55*, 2471.
(37) Parr, R. G.; Yang, W. *Density Functional Theory of Atoms and Molecules*; Oxford University Press: New York, 1989.
(38) Becke, A. D. *Phys. Rev. A* **1988**, *38*, 3098.
(39) Lee, C.; Yang, W.; Parr, R. G. *Phys. Rev. B* **1988**, *37*, 785.
(40) Marx, D.; Hutter, J. In *Modern Methods and Algorithms of Quantum Chemistry, NIC Series Vol.1*; Grotendorst, J., Ed.; John von Neuman Institut für Computing: Forschungszentrum, Jülich, 2000; pp 301−449.
(41) Tuckerman, M. E. *J. Phys.: Condens. Matter* **2002**, *14*, R1297.
(42) Tuckerman, M. E.; Yarne, D. A.; Samuelson, S. O.; Hughes, A. L.; Martyna, G. J. *Comput. Phys. Commun.* **2000**, *128*, 333.
(43) Hohenberg, P.; Kohn, W. *Phys. Rev.* **1964**, *136*, B864.
(44) Kohn, W.; Sham, L. J. *Phys. Rev.* **1965**, *140*, A1133.
(45) Laasonen, K.; Sprik, M.; Parrinello, M.; Car, R. *J. Chem. Phys.* **1993**, *99*, 9080.
(46) Tuckerman, M. E.; Laasonen, K.; Sprik, M.; Parrinello, M. *J. Chem. Phys.* **1995**, *103*, 150.
(47) Silvestrelli, P. L.; Parrinello, M. *J. Chem. Phys.* **1999**, *111*, 3572.
(48) Marx, D.; Tuckerman, M. E.; Hutter, J.; Parrinello, M. *Nature* **1999**, *397*, 601.
(49) Tuckerman, M.; Marx, D.; Parrinello, M. *Nature* **2002**, *417*, 925.
(50) Zhu, Z.; Tuckerman, M. E. *J. Phys. Chem. B* **2002**, *106*, 8009.
(51) Chen, B.; Ivanov, I.; Park, J. M.; Parrinello, M.; Klein, M. L. *J. Phys. Chem. B* **2002**, *106*, 12006.
(52) Chen, B.; Park, J. M.; Ivanov, I.; Tabacchi, G.; Klein, M. L.; Parrinello, M. *J. Am. Chem. Soc.* **2002**, *124*, 8534.
(53) Tuckerman, M.; Chandra, A.; Marx, D. *Acc. Chem. Res.* **2006**, *39*, 151.
(54) Lee, H.-S.; Tuckerman, M. E. *J. Chem. Phys.* **2006**, *125*, 154507.
(55) Chandra, A.; Tuckerman, M. E.; Marx, D. *Phys. Rev. Lett.* **2007**, *99*, 145901.
(56) Lee, H.-S.; Tuckerman, M. E. *J. Chem. Phys.* **2007**, *126*, 164501.
(57) Troullier, N.; Martins, J. L. *Phys. Rev. B* **1991**, *43*, 1993.
(58) Minary, P.; Tuckerman, M. E.; Pihakari, K. A.; Martyna, G. J. *J. Chem. Phys.* **2002**, *116*, 5351.
(59) Martyna, G. J.; Klein, M. L.; Tuckerman, M. E. *J. Chem. Phys.* **1992**, *97*, 2635.
(60) Carter, E. A.; Ciccotti, G.; Hynes, J. T.; Kapral, R. *Chem. Phys. Lett.* **1989**, *156*, 472.
(61) Sprik, M.; Ciccotti, G. *J. Chem. Phys.* **1998**, *109*, 7737.
(62) Wilson, M. A.; Pohorille, A.; Pratt, L. R. *J. Phys. Chem.* **1987**, *91*, 4873.
(63) Kuo, I. F. W.; Mundy, C. J. *Science* **2004**, *303*, 658.
(64) Yeh, I.-C.; Hummer, G. *J. Phys. Chem. B* **2004**, *108*, 15873.
(65) Kuo, I. F. W.; Mundy, C. J.; Eggimann, B. L.; McGrath, M. J.; Siepmann, J. I.; Chen, B.; Vieceli, J.; Tobias, D. J. *J. Phys. Chem. B* **2006**, *110*, 3738.
(66) McGrath, M. J.; Siepmann, J. I.; Kuo, I. F. W.; Mundy, C. J.; VandeVondele, J.; Hutter, J.; Mohamed, F.; Krack, M. *Chem. Phys. Chem.* **2005**, *6*, 1894.
(67) McGrath, M. J.; Siepmann, J. I.; Kuo, I. F. W.; Mundy, C. J.; VandeVondele, J.; Hutter, J.; Mohamed, F.; Krack, M. *J. Phys. Chem. A* **2006**, *110*, 640.
(68) McGrath, M. J.; Siepmann, J. I.; Kuo, I. F. W.; Mundy, C. J. *Mol. Phys.* **2006**, *104*, 3619.
(69) Shultz, M. J.; Baldelli, S.; Schnitzer, C.; Simonelli, D. *J. Phys. Chem. B* **2002**, *106*, 5313.
(70) Brown, E. C.; Mucha, M.; Jungwirth, P.; Tobias, D. J. *J. Phys. Chem. B* **2005**, *109*, 7934.

JP809236C